Photochemical Coenzyme Regeneration in an Enzymatically Active Optical Material

Jenna L. Rickus,[†,§] Pauline L. Chang,[‡] Allan J. Tobin,[#] Jeffrey I. Zink,[⊥] and Bruce Dunn*[,||]

Departments of Chemistry and Biochemistry, Materials Science and Engineering, Chemical Engineering, Neurobiology, Physiological Sciences, Brain Research Institute, Neuroscience IDP Neuroengineering Program, University of California, Los Angeles, Los Angeles, California 90095

Received: December 30, 2003; In Final Form: April 15, 2004

The photoinduced electron transfer between immobilized thionine and the dinucleotide enzyme cofactors NADH and NADPH in a SiO_2 sol−gel matrix is reported. The electron-transfer quenching of thionine luminescence is used to monitor the rate of NADPH oxidation. Using Stern−Volmer quenching curves, the quenching rates in the silica matrix are 1 to 2 orders of magnitude smaller than those in solution. The rate constants for oxidation of NADPH by thionine were measured to be $9.8(\pm 2.9) \times 10^{-3}$ s^{-1} in solution and $8.8(\pm 1.0) \times 10^{-4}$ s^{-1} in the gel. Within the silica matrix, the photoinduced oxidation of NADPH is combined with the enzymatic reaction of isocitrate dehydrogenase, which uses the oxidized cofactor, $NADP^+$, as an electron acceptor in the oxidation of isocitrate. The encapsulated isocitrate dehydrogenase is active with a Michaelis−Menten constant, K_M, of 3 μM and a k_{cat} of 0.67 μM/s per mg_{enzyme}. Because optical sensors use NADPH fluorescence as an indicator of the presence and relative concentration of enzyme substrate, the successful demonstration of photoinduced regeneration of $NADP^+$ makes possible continuous monitoring by the family of dehydrogenase enzymes.

1. Introduction

The specificity and selectivity of enzymes make them important components for sensor applications. For optical sensing, enzymes that use NAD or NADP as enzyme cofactors are particularly important because the reduced cofactors fluoresce. This property makes these enzymatic reactions particularly useful for solid-state and fiber optic based systems, as the enzyme−coenzyme is able to provide both molecular recognition and signal transduction. Optical sensors take advantage of the NADH or NADPH fluorescence as an optical indicator of the presence and relative concentration of enzyme substrate.[1] The largest class of redox enzymes that utilize NAD or NADP as the enzyme cofactor are the dehydrogenases that carry out the general reaction

$$\text{reduced substrate} + \text{NAD(P)}^+ \rightarrow \text{oxidized substrate} + \text{NAD(P)H} + \text{H}^+ \quad (1)$$

This reaction consumes the oxidized form of the coenzyme. Sensors based on this reaction cannot operate continuously without an external supply of coenzyme.

The objective of the research in this paper is to determine whether a photooxidizer can be incorporated in the same solid-state matrix as the enzyme and cofactor to regenerate, by oxidation, the reduced cofactor. For the photooxidation process to be successful, several criteria need to be met. The photooxidizer must be incorporated in the same matrix as that of the other components, i.e., co-immobilized with the enzyme and the enzyme cofactor. It must be stable in this matrix and retain its excited-state properties. In addition, the photooxidizer must be compatible with the other components and unreactive.

We have chosen 3,7-diamino-5-phenothiazinium acetate, thionine or $thio^+$, as the photooxidizing agent because it meets the above criteria. In solution, excited thionine oxidizes NADH[2,3] and we expect that it will also oxidize NADPH. Thionine, $thio^+$, absorbs light in the visible range, $\lambda_{max} = 596$ nm (reaction 2). The excited molecule, $^*thio^+$, can return to the ground state via nonradiative processes (reaction 3) or fluorescence (reaction 4).[4] In the presence of NADH, electron transfer that oxidizes NADH competes with the fluorescence and quenches the thionine emission. In this paper we use reaction 5 to regenerate the oxidized form of the enzyme cofactor that was depleted by the enzyme reaction (reaction 1).

$$\text{thio}^+ + h\nu_{596} \xrightarrow{k_d} {}^*\text{thio}^+ \quad (2)$$

$${}^*\text{thio}^+ \xrightarrow{k_d} \text{thio}^+ \quad (3)$$

$${}^*\text{thio}^+ \xrightarrow{k_f} \text{thio}^+ + h\nu_{620} \quad (4)$$

$${}^*\text{thio}^+ + \text{NADH} \xrightarrow{k_q} \text{thio} + \text{NAD}^+ \quad (5)$$

The enzyme isocitrate dehydrogenase (ICDH) was selected as a representative dehydrogenase. ICDH catalyzes the oxidation of isocitrate to α-ketoglutarate, using $NADP^+$ as the electron acceptor (reaction 6).

$$\text{isocitrate} + \text{NAD(P)}^+ \rightarrow \text{α-ketoglutarate} + \text{CO}_2 + \text{NAD(P)H} + \text{H}^+ \quad (6)$$

While most dehydrogenase reactions are reversible, the change

* Address correspondence to this author. E-mail: bdunn@ucla.edu.
† Neuroscience IDP Neuroengineering Program.
§ Present address: Department of Agricultural and Biological Engineering, Department of Biomedical Engineering, Purdue University, West Lafayette, IN 47907.
‡ Chemical Engineering.
# Neurobiology, Physiological Science, Brain Research Institute.
⊥ Chemistry and Biochemistry.
|| Materials Science and Engineering.

10.1021/jp038051g CCC: $27.50
Published on Web 05/26/2004

in Gibbs free energy of the ICDH reaction strongly favors the oxidation of isocitrate, thereby reducing experimental complications from back reactions.[5]

When thionine is co-immobilized with the enzyme, the NADPH produced by ICDH in the presence of isocitrate should be converted back to $NADP^+$ when the gel is exposed to visible light. Excitation of the co-immobilized thionine should allow for a self-sustaining supply of $NADP^+$ for further isocitrate oxidation.

The matrix we selected for study is sol−gel derived silica. The sol−gel process leads to a transparent, porous glass that is formed at room temperature and is able to physically immobilize a wide variety of molecules.[6−10] Of particular relevance for the present work is the immobilization of dehydrogenases including glucose dehydrogenase,[10−12] lactate dehydrogenase,[13−15] and alcohol dehydrogenase.[16,17] In all of these examples, the enzyme cofactor (NAD^+ or $NADP^+$) used in the transduction was consumed and not regenerated.

In this paper, we first show that NADPH is oxidized by photoexcited thionine. The oxidations of the cofactors, NADH and NADPH, are compared both in a silica sol−gel matrix and in solution. The rates are characterized by steady-state quenching experiments and by fluorescence measurements. Second, ICDH is encapsulated in the sol−gel matrix and the kinetics of the encapsulated enzyme are characterized. Finally, the thionine−NADPH reaction is used to regenerate the $NADP^+$ that was consumed in the enzymatic oxidation of isocitrate by isocitrate dehydrogenase. All the components were immobilized in the optically transparent silica gel matrix. The result is a solid-state system capable of being regenerated by light.

2. Experimental Methods

2.1. Materials Synthesis. NAD^+, $NADP^+$, NADH, NADPH, isocitrate dehydrogenase, and isocitrate were all purchased from Sigma. Thionine acetate and tetramethoxysilane (TMOS) were purchased from Fluka. All chemicals were used as purchased. A 100 μM stock solution of thionine was prepared by dissolving thionine in buffer (0.02 M sodium phosphate, 0.02 M NaCl, pH 7) and sonicating it for 10 min.

TMOS was hydrolyzed by sonication in water (silica:water molar ratio of ∼1:2) and 0.5 mM HCl for 15 min. The hydrolyzed TMOS sol was combined with buffer (0.02 or 0.1 M sodium phosphate, 0.02 or 0.1 M sodium chloride, pH 7.0) in a 2:3 volumetric ratio. Emission spectra samples were cast into 4.5 mL of polystyrene cuvettes, covered with Parafilm and foil, and aged for 24 h. For kinetic fluorescence measurements, 100 μL of doped sol was cast into the wells of a 96-well Nunc microplate. Dopants (thionine, NADH, or ICDH) were added to the buffer prior to the addition of TMOS sol. Gels were covered with a small volume of buffer to prevent drying during the aging time. Drying leads to slow kinetics and therefore only aged wet gels were investigated. Thionine- and NADH-doped monoliths were aged for 1 h at room temperature. ICDH-doped monoliths (240 ng/100 μL) were aged for 24 h at 4 °C. Solution controls were made for comparison by adding buffer in place of hydrolyzed TMOS.

2.2. Spectroscopic Measurements. Fluorescence emission spectra were taken with a SPEX Fluorolog spectrometer with a right angle configuration. Samples were excited at 590 nm and emission intensity was measured from 610 to 700 nm. Measurements were taken in the same polystyrene cuvettes in which the gels were prepared. Only minimal shrinkage of the gels occurred over the 24-h aging period.

2.3. Kinetic Experiments. Time-resolved fluorescence measurements were taken with a Fluoroskan Ascent microplate fluorometer. Excitation and emission wavelengths for NADH and NADPH were 355 and 460 nm. Excitation and emission wavelengths for thionine were 584 and 620 nm. NADH and NADPH fluorescence was measured with an integration time of 20 ms while thionine fluorescence was measured with an integration time of 100 ms.

Steady-state quenching experiments were conducted with thionine-doped gels and thionine solutions with final concentrations of 8 and 5 μM, respectively. At $t = 0$, 20 μL of NADPH or NADH was injected into the sample well, and thionine fluorescence was measured over time. Co-encapsulation of the coenzyme and thionine was not practical because coenzyme oxidation occurred during the gelation period. For all samples the quenched intensity ratio, I_0/I, was defined as the average intensity in the absence of quencher divided by the intensity minimum at steady state after the injection of NADH or NADPH.

For NADH and NADPH oxidation experiments, gel and solution samples with final NADPH concentrations of 33, 66, and 100 μM were produced in triplicate. At $t = 0$, 20 μL of 60 μM thionine was injected into each sample. Thionine was excited over five intervals of 200 s, and the thionine fluorescence emission was collected during each interval. NADPH fluorescence was measured before and after each thionine excitation interval.

For enzyme characterization experiments, ICDH-doped gels (240 ng/100 μL) were produced and aged for 24 h at 4 °C. Kinetic experiments were conducted in the same 96-well plate in which the gels were prepared. The gels were allowed to equilibrate in a phosphate-buffered solution of $NADP^+$, so that the final cofactor concentration of $NADP^+$ was 2.67 mM. Isocitrate was injected into each well at varying concentrations at time = 0. The production of NADPH by the enzyme over time was determined by measuring NADPH fluorescence over time. NADPH fluorescence was converted to NADPH concentration with use of a linear calibration curve (data not shown). The initial reaction velocity was estimated by fitting the linear portion of the fluorescence increase near time zero with least-squares methods.

The reaction of thionine with NADPH was coupled to the enzyme reaction of isocitrate dehydrogenase (ICDH) by producing samples codoped with thionine and ICDH (144 ng/100 μL). Samples were incubated with $NADP^+$ so that the final enzyme cofactor concentration was 16 mM. At time = 0, 40 μL of 4 mM isocitrate was injected into the sample well. NADPH production by ICDH was measured by fluorescence for ∼1600 s. The thionine was then excited at 584 nm for 200 s. Three NADPH fluorescence measurements were made during the thionine excitation period. Following the thionine excitation period, isocitrate was again injected into the sample well. The NADPH fluorescence again was measured for 1600 s, and thionine was excited for 200 s. This process was repeated 2 more times without any washing steps.

3. Results and Discussion

3.1. Enzyme Cofactor Regeneration Scheme. The goal of this work is to establish and characterize the oxidation of NADPH with excited thionine within the pores of a silica matrix, and to then couple this excited-state redox reaction to the enzymatic reduction of NADPH by ICDH. Figure 1 illustrates how the coupling of these reactions could be used for the continuous sensing of isocitrate. As isocitrate is oxidized to

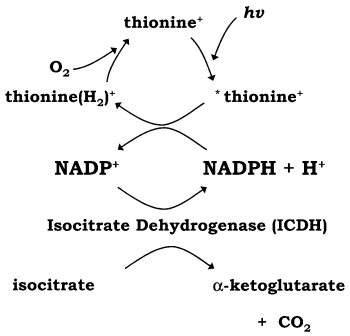

Figure 1. Enzyme cofactor regeneration for continuous isocitrate oxidation. The photochemical oxidation of NADPH by thionine is coupled to the enzyme reaction of isocitrate dehydrogenase (ICDH). ICDH oxidizes isocitrate to α-ketoglutarate, using $NADP^+$ as the electron acceptor. When thionine is excited, it reacts with NADPH to reform $NADP^+$. The regenerated $NADP^+$ can participate in another round of isocitrate oxidation.

α-ketoglutarate by ICDH, $NADP^+$ is reduced to NADPH. If the resulting NADPH can be converted back to $NADP^+$ by excited thionine, then the cofactor can again participate in the enzyme reaction. This system would have a self-sustaining enzyme cofactor source for ongoing isocitrate detection (in the presence of oxygen) without requiring additional reagents. Only light need be supplied to the sensor material.

3.2. Formation of Doped Glasses. All glasses were formed by using the sol−gel method described previously for encapsulating proteins while retaining the biological activity of the protein.[18,19] The precursor tetramethoxysilane, TMOS, is hydrolyzed under acidic conditions in a sonication bath. The addition of phosphate buffer to the resulting hydrolyzed sol increases the pH to promote condensation of the precursor to form a three-dimensional porous gel. Because the dopant molecule is introduced with the buffer, it is protected from the harsh environment of the acidic sol.

In this work, thionine-doped gels, ICDH-doped gels, and thionine/ICDH codoped gels are all synthesized. Gelation occurred within 1 min, producing clear gels that were either deep purple or colorless depending on the presence or absence of thionine. Characterization of the reaction between encapsulated thionine and NADH/NADPH in this "protein-friendly" glass allowed the reaction to then be coupled to the ICDH reaction in the same material by codoping gels with both thionine and the enzyme.

3.3. ICDH Enzyme Kinetics in Aged Gels. Many enzymes follow a steady-state Michaelis−Menten kinetic model in solution.[5] The model is described by the Michaelis−Menten equation where V_o is the initial reaction velocity, [S] is the initial substrate concentration, V_{max} is the maximum reaction velocity, and K_M is the Michaelis−Menten constant (eq 7). The equation results in two parameters that characterize the kinetics of the reaction. The initial velocity of the reaction (the reaction velocity before any significant product accumulation occurs) increases with substrate concentration and approaches a maximum velocity, V_{max}, as the enzyme becomes saturated with substrate. The Michaelis−Menten constant, K_M, is the substrate concentration at which the reaction occurs at half the maximum velocity.

$$V_o = \frac{V_{max}[S]}{K_M + [S]} \tag{7}$$

Encapsulated enzymes also often follow similar kinetics. However, if diffusion limitations are present, the characteristic constants are apparent constants rather than intrinsic ones. The values of these constants include diffusion and geometric parameters as well as the intrinsic kinetic parameters of the enzyme.[20,21]

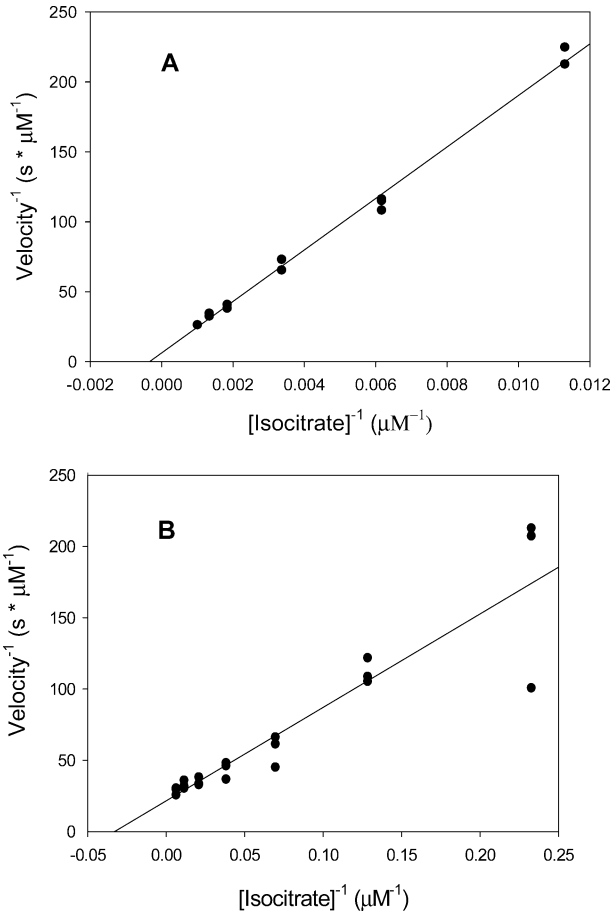

Figure 2. Lineweaver−Burke plot of ICDH after encapsulation in aged gels (A) and in free solution (B). The inverse of the initial velocity of the reaction is plotted against the inverse of the initial isocitrate concentration. A linear fit of the data to the Michaelis−Menten constant results in a K_M of 3 μM and a V_{max} of 0.17 μM/s for the encapsulated enzyme and a K_M of 29 μM and a V_{max} of 0.05 μM/s for the free enzyme.

To evaluate ICDH as a model dehydrogenase for co-encapsulation with thionine, we produced ICDH-doped gels and measured their response to varying isocitrate concentrations at saturating $NADP^+$ levels. Isocitrate was injected onto each sample, and the ICDH reaction was monitored via the production of NADPH. For each sample tested, NADPH fluorescence increased with time after isocitrate injection and then leveled off to a final steady value as is expected for an enzyme reaction. Figure 2 shows the initial velocity of each reaction as a function of the initial isocitrate concentration. The inverse of the initial velocity correlates linearly with the inverse of the initial isocitrate concentration as is predicted by the Michaelis−Menten equation. A linear fit results in a Michaelis−Menten constant, K_M, of 3 μM and a maximum initial velocity, V_{max}, of 0.17 μM/s. The strong correlation between reaction velocity and isocitrate concentration demonstrates both the activity of the encapsulated ICDH and the material's ability to distinguish between different isocitrate concentrations in a predictable manor.

For comparison, ICDH samples in buffer solution were also evaluated at the same isocitrate concentrations and the same saturating $NADP^+$ concentration. Again an increase in NADPH fluorescence was observed for each sample after the addition

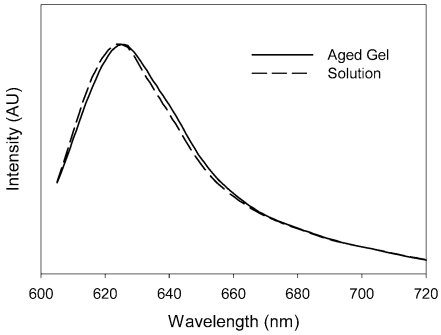

Figure 3. Fluorescence emission spectra of thionine in buffer solution and thionine encapsulated in aged silica gels. The samples were excited at 590 nm.

of isocitrate. A linear fit to the Michaelis−Menten equation resulted in a K_M of 29 μM and a V_{max} of 0.05 μM/s. The change in the K_M after encapsulation may be a result of diffusion limitations, changes in the local pH or ion concentrations, or changes in binding affinity of the enzyme for the substrate. Because V_{max} is a linear function of enzyme concentration, the measured values must be adjusted for enzyme concentration to compare the maximum catalytic rates, k_{cat}, of the encapsulated and free enzyme. The k_{cat} for the encapsulated enzyme was 0.67 μM/s per mg_{enzyme} while the k_{cat} for the free enzyme was 3.8 μM/s per mg_{enzyme}. The catalytic and binding rates are often reduced for encapsulated enzymes compared to free enzyme in solution.[22−25] As the kinetic measurements were conducted in bulk gel materials, it is likely that diffusion is contributing significantly to the reduction in k_{cat}.

3.4. Emission Spectra of Thionine-Doped Gels. Comparison of thionine emission spectra in solution and in the sol−gel environment reveals almost no difference between the two (Figure 3). The fluorescence emission peak for 20 μM thionine in the gel is at 624 nm and is slightly red shifted to 626 nm for 40 μM thionine gels. A red shift with increasing thionine concentration is consistent with behavior in aqueous solution and with previous work.[26] While it is known that thionine tends to dimerize in water ($K_{dimer} = 4 \times 10^3$ M^{-1}),[27] there is no discernible second peak at 665 nm, indicating that thionine dimers are not a significant factor in the gels.[26]

3.5. Quenching in Solution and in Aged Gels. NADH has been shown to quench thionine fluorescence in aqueous solution in a reaction that results in the net production of NAD^+.[2,3] To determine whether NADPH undergoes a reaction similar to that of NADH with thionine, we examined their relative abilities to quench thionine fluorescence. Thionine in phosphate buffer was exposed to varying concentrations of NADPH or NADH. The thionine fluorescence intensity was measured as a function of time. After addition of NADPH or NADH, the thionine fluorescence decreased quickly to a new pseudo-steady-state value. Given enough time, however, the thionine fluorescence returned to baseline, indicating thionine was not consumed during the reaction, but merely quenched.

In homogeneous media, quenching can be described with steady-state Stern−Volmer kinetics:

$$\frac{\tau_o}{\tau} = 1 + K_{SV}[Q] \tag{8}$$

$$K_{SV} = k_q \tau_o \tag{9}$$

where K_{SV} is the Stern−Volmer constant (M^{-1}), [Q] is the concentration of quencher (M), k_q is the bimolecular quenching rate constant (M^{-1} s^{-1}), τ_o is the fluorescence lifetime of thionine in the absence of quencher, and τ is the fluorescence lifetime in the presence of quencher.

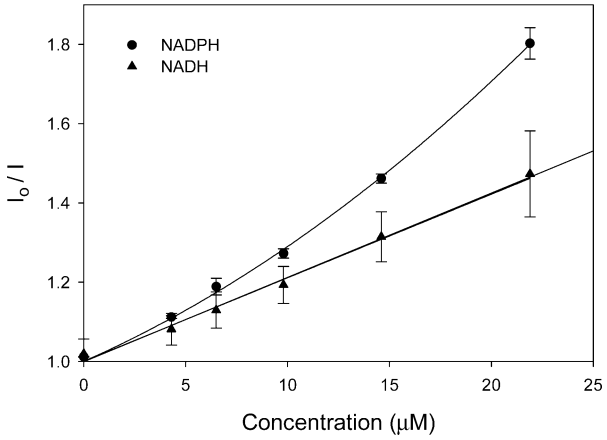

Figure 4. Quenching curves for thionine by NADPH and NADH in phosphate buffer solution. Steady-state intensity ratios for thionine in buffer solution are plotted as a function of cofactor concentration. A linear regression of the thionine intensities as a function of NADH concentration resulted in a fit function of $I_o/I = 1 + (2.1 \times 10^{-2})$[NADH], r2 = 0.99. A nonlinear regression of the thionine intensities as a function of NADPH concentration resulted in a fit function of $I_o/I = (6.4 \times 10^{-4})$[NADPH]$^2 + (2.3 \times 10^{-2})$[NADPH] + 1, r2 = 0.99.

In the case of pure dynamic quenching, the relative reduction in emission intensity is equal to the relative reduction in the fluorescence lifetime, and the relationship between relative intensity and quencher concentration is linear:

$$\frac{I_o}{I} = \frac{\tau_o}{\tau} = 1 + K_{SV}[Q] \tag{10}$$

where I_o is the fluorescence intensity in the absence of quencher and I is the fluorescence intensity in the presence of quencher.

However, when static quenching mechanisms also occur through the complexing of the ground state donor and quencher molecules, the relative reduction in emission intensity is greater than the relative reduction in fluorescence lifetime. In this case a quadratic relationship between relative intensity and quencher concentration is predicted:

$$\frac{I_o}{I} = 1 + (K_{SV} + K_{eq})[Q] + K_{eq}K_{SV}[Q]^2 \tag{11}$$

where K_{eq} is the equilibrium constant for the binding of the donor and quencher.

The quenching experiment for NADH and thionine in solution was repeated three times to provide a better estimate of the Stern−Volmer and quenching rate constants for the reaction. The K_{SV} was estimated to be $4.5(\pm 0.8) \times 10^4$ M^{-1} based on the slopes of three quenching curves including the one shown in Figure 4. This estimate is consistent with that previously reported by Sharma and Arnold, $6.2(\pm 0.2) \times 10^4$ M^{-1}.[2]

Figure 4 shows that I_o/I for thionine increased linearly with NADH concentration as is predicted by the Stern−Volmer relation (eq 10) for steady-state dynamic quenching. However, the quenching rate constant, k_q, that is calculated from the measured Stern−Volmer constant $(1.4(\pm 0.3) \times 10^{14}$ M^{-1} s^{-1}, using a thionine florescence lifetime, τ_o, of $320(\pm 20) \times 10^{-12}$ s) is faster than what is possible for diffusion-controlled reactions.[4] The large magnitude of the estimated k_q is consistent with literature values and indicates that some level of static quenching must also be occurring.[2] Nonlinearities in the

quencher curve, however, are not apparent for NADH. Evidence for the formation of complexes between thionine and other mono- and polynucleotides also supports a static quenching process.[28,29]

The quenching curve for NADPH, on the other hand, is nonlinear and is better fit by a quadratic function than a linear one (Figure 4). This difference indicates that static mechanisms may be playing a larger role in the quenching of thionine by NADPH than by NADH. It is possible that the addition of the phosphate group may change the binding constant of the dinucleotide and thionine.

The quenching experiments were repeated for immobilized thionine in silica gels. The shape of the quenching curves changed after immobilization to a nonlinear relationship with a downward curvature (Figure 5a,b). This is consistent with observations from other immobilized systems using a heterogeneous matrix.[30,31] Such quenching curves are typically fit with a two-site model function (eq 12) or by a power-law function (eq 13).[30] The quencher curves for NADH and NADPH in Figure 5 were fit by using the power-law function.

$$\frac{I_o}{I} = \frac{1}{\dfrac{f_{01}}{1 + K_{SV1}[Q]} + \dfrac{f_{02}}{1 + K_{SV2}[Q]}} \tag{12}$$

$$\frac{I_o}{I} = 1 + a[Q]^b \tag{13}$$

The two-site model assumes two discrete subpopulations of fluorphore where the f_{0i} values are the fraction of emission from each subpopulation and the K_{SVi} values are the Stern−Volmer constants for each subpopulation.[32] Each subpopulation interacts differently with the matrix and therefore has a different K_{SV}. This model can also be expanded to a multisite model or distribution model that assumes a higher number of discrete populations or a distribution of dopant populations.[31] The power-law function has no physical correlate; a and b are simply fitting parameters. This relationship, however, can be useful in the design and calibration of sensors despite its lack of physical meaning.

A comparison of the quenching curves for the cofactors in solution (Figure 4) and in the gel (Figure 5) reveals that between 1 and 2 orders of magnitude more cofactor is required to achieve the same level of quenching in the gel compared to solution.

As the dinucleotides were added after the formation of the gels, one possible explanation for the reduction in the observed K_{SV} is pore exclusion of the dinucleotides. Charged molecules can be partially excluded from the pore interior at low ionic strengths such as those used in these experiments.[33] The quencher plots were constructed assuming that the concentration of enzyme cofactor in the pores was equal to the concentration in bulk. It is likely that the negatively charged enzyme cofactor may not fully penetrate the sol−gel pores resulting in a lower concentration than assumed. If the concentration of the coenzyme is lower in the gel than in solution, then the observed quenching rates in Figure 5 represent a lower limit. This would result in a shift in the quenching curves to higher bulk concentrations.

In addition, the matrix structure could be decreasing the effective quenching rate by interacting with thionine in such a way as to decrease the population that is able to interact with cofactor. This is consistent with the multisite model, which is based on an interpretation involving subpopulations of thionine with reduced quenching rates. The reduction could be due to the physical constraint of a subpopulation of molecules in confining regions that have restricted access to the bulk solution and therefore not participate in the electron transfer.[34] In addition, a second subpopulation of thionine molecules close to the silica pore interface could have a reduced quenching rate due to interactions such as electrostatic adhesion to the wall.[7,33] This type of interaction could reduce both dynamic processes through a reduction in collision rate as well as static processes through a reduction in nucleotide binding. Although not shown here, leaching experiments conducted in the same buffer and ionic strength reveal that there is, in fact, a strong interaction between the dye and the surface of the glass. Only small amounts of thionine leach from doped gels even with lengthy and repeated washes.

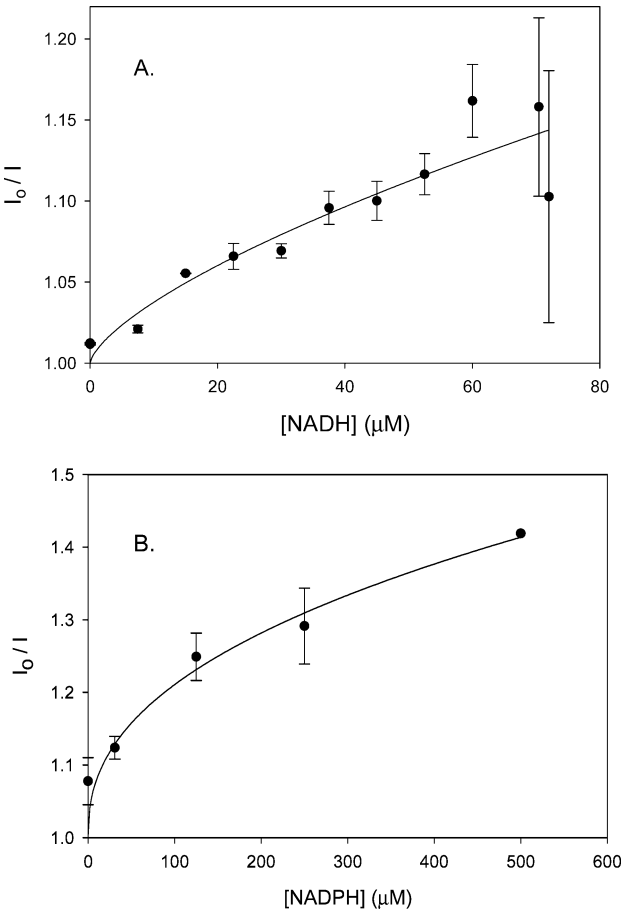

Figure 5. Quenching curves for encapsulated thionine by NADH (A) and NADPH (B) in silica gels. The thionine fluorescence intensity ratio is plotted as a function of cofactor quencher concentration in aged gels. Both plots were fit to the power function, $I_o/I = 1 + a[Q]^b$. For NADH, $a = 7.8 \times 10^{-3}$ and $b = 0.68$ with r2 = 0.87. For NADPH, $a = 3.1 \times 10^{-2}$ and $b = 0.42$ with r2 = 0.91.

Although the quenching rates for the encapsulated system are 1 to 2 orders of magnitude slower than those for solution, this reduction would still result in k_q values that are faster than what is expected for diffusion-controlled reactions, indicating that static quenching mechanisms are still playing a role after encapsulation.

3.6. NADPH Oxidation Rates. When thionine was exposed to NADPH, its fluorescence was quenched to a constant value. Given enough time, however, the thionine fluorescence levels returned to initial levels suggesting that thionine was not consumed during the quenching. The return of the thionine levels to baseline signifies the disappearance of the quenching reaction due to a depletion of NADPH concentration. To validate and

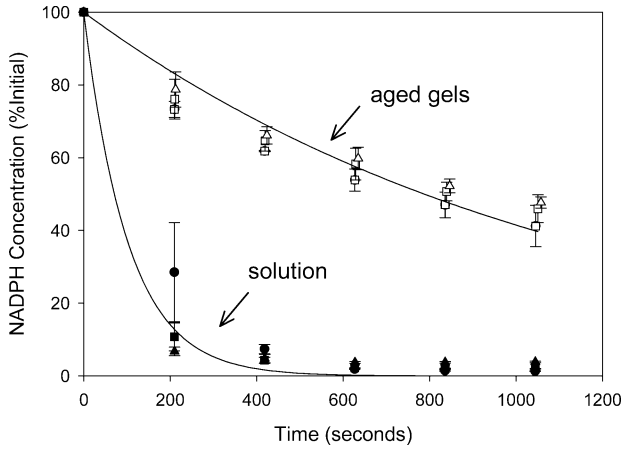

Figure 6. Disappearance of NADPH during exposure to excited thionine in buffer solution and in aged gels. NADPH levels, measured via NADPH fluorescence intensity, are plotted as a function of exposure time. The NADPH concentration is expressed as a percentage of the initial NADPH concentration at time = 0. Open symbols show the decrease of NADPH in aged gels. Closed symbols show the decrease of NADPH in solution. Three starting NADPH concentrations were used for each sample type: ○, aged gel, 120 μM NADPH; □, aged gel, 80 μM NADPH; △, aged gel, 40 μM; ●, buffer solution, 120 μM NADPH; ■, buffer solution, 80 μM NADPH; ▲, buffer solution, 40 μM NADPH. The data for the six conditions were fit individually to a single-exponential decay, $y = 100e^{-bt}$. The decay parameter, *b*, for the aged gels and the solution samples was $8.8(\pm1.0) \times 10^{-4}$ and $9.8(\pm2.9) \times 10^{-3}$ s^{-1} respectively. The r2 for each fit ranged between 0.86 and 0.99 with a mean of 0.97.

characterize the consumption of NADPH, we monitored the NADPH fluorescence levels during the quenching of thionine. When NADPH-doped gels and NADPH solutions were exposed to excited thionine, the NADPH fluorescence decreased with time, but unlike thionine, the NADPH fluorescence levels did not return to baseline. These results validate that NADPH is consumed in the quenching reaction with thionine, as is the case with NADH in solution.[2,3]

Figure 6 shows the NADPH concentration, expressed as a percentage of the initial NADPH concentration, over time in the presence of excited thionine. NADPH fluorescence is linearly proportional to concentration within the range used. The thionine fluorescence quickly dropped to a reduced level and remained relatively constant for the duration of the reaction. For a constant $*thio^+$ level, the NADPH consumption would be expected to follow a single-exponential decay (eqs 14 and 15) with a pseudo-first-order decay constant, $k_{oxidize}$, equal to the product of the quenching constant, k_q, and $[*thio^+]$. The data were fit to an exponential decay function and the $k_{oxidize}$ was estimated for each sample.

$$\frac{d[NADPH]}{dt} = k_{oxidize}[NADPH(t)] \quad (14)$$

$$[NADPH(t)] = [NADPH(t=0)]e^{-k_{oxidize}} \quad (15)$$

The rate of disappearance of NADPH is 1 order of magnitude slower in the sol−gel, $k_{oxidize} = 8.8(\pm1.0) \times 10^{-4}$ s^{-1}, compared with solution, $k_{oxidize} = 9.8(\pm2.9) \times 10^{-3}$ s^{-1}. This rate reduction is consistent with the rate reduction seen in the steady-state quenching experiments. In this case, however, the cofactor was immobilized and the thionine was diffused into the gel. Thionine is positively charged and is likely to have strong interactions with the negatively charged silica matrix, which makes pore exclusion a less likely contributor to reduced rates. It is possible that diffusion restrictions are playing a role in the decrease in observed reaction rate. From reaction rates alone, it is impossible to determine the individual contributions of diffusion barriers, pore exclusion, and multiple dopant populations.

3.7. Reaction Mechanism. While the presented oxidation experiments address the consumption of NADPH, they do not directly confirm the production of $NADP^+$. However, data reported elsewhere by us and by Sharma have verified that the reaction product of excited thionine and NADH and NADPH is NAD^+ and $NADP^+$, respectively, by its ability to act as an electron acceptor in NAD^+ or $NADP^+$ specific enzyme reactions.[35−37] These results indicate that the quenching of thionine is at least partially due to an excited-state redox process that results in a net electron transfer from NADH or NADPH to thionine.

Although the exact mechanism for thionine quenching by NAD(P)H is not known, it has been suggested that short-lived semithionine, $thio(H)^+$, and leukothionine, $thio(H_2)^+$, intermediates are likely (reactions 16 and 17).[3]

$$*thio^+ + NADPH + H^+ \rightarrow thio(H_2)^+ + NADP^+ \quad (16)$$

$$2*thio^+ + NADPH + H^+ \rightarrow 2thio(H)^+ + NADP^+ \quad (17)$$

$$2thio(H_2)^+ + O_2 \rightarrow 2H_2O + 2thio^+ \quad (18)$$

$$4thio(H)^+ + O_2 \rightarrow 2H_2O + 4thio^+ \quad (19)$$

Two electrons must be removed from NADPH to form $NADP^+$. Reaction 16 would result if both electrons were accepted by one thionine molecule, whereas reaction 17 would result if the two electrons were accepted by two different thionine molecules. The samples in this study were not deoxygenated and the suggested nonfluorescent intermediates are likely to be quickly converted back to ground-state thionine through reaction with oxygen in the solution (reactions 18 and 19).

In addition, because the quenching rate of thionine is much faster that the rate of disappearance of NADPH or NADH, we suggest that the electron transfer between thionine and enzyme cofactor is reversible. Only a fraction of the electron-transfer events result in a net production of oxidized cofactor, but thionine fluorescence is quenched each time regardless of the presence of the back reaction.

NADH and NADPH are dinucleotide cofactors with one nicotinamide base and one adenine base. Adenine nucleotides have been shown to quench thionine fluorescence while the site of NADH and NADPH oxidization is on the nicotinamide ring.[5,28] It is therefore possible that the dinucleotide has two sites of interaction with thionine and that the adenine nucleotide can quench thionine independent from the cofactor oxidation reaction. To investigate this possibility we have measured the quenching rate of thionine by adenosine 5′-monphosphate (AMP) using the same steady-state methods presented here and have found the k_q to be 3 orders of magnitude smaller than for NADH or NADPH. This result is consistent with literature values and suggests that the quenching by the adenine nucleotide is secondary to the interaction at the nicotinamide site.[28]

3.8 Reaction Coupling. Figure 1 illustrated how the photochemical oxidation of NADPH can be coupled to the enzymatic oxidation of isocitrate. ICDH was chosen as the model dehydrogenase because the change in Gibbs free energy of the reaction greatly favors the forward oxidation reaction.[38] The lack of a significant reverse reaction allows for the ICDH reaction to go close to completion before starting the regenera-

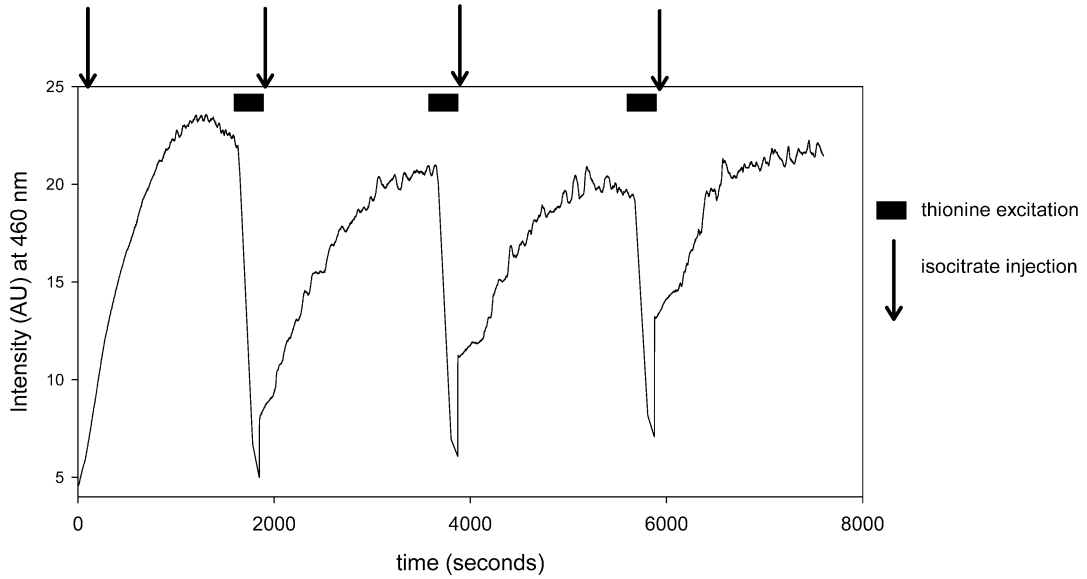

Figure 7. Repeated ICDH reactions in a sol−gel monolith. ICDH, thionine, and $NADP^+$ are encapsulated in a silica gel. Isocitrate is injected onto the gel (at times indicated by arrows) and the reaction is monitored via NADPH fluorescence. After each reaction thionine is excited (at times indicated by solid bars) to induce the oxidation of NADPH back to $NADP^+$. After the NADPH levels have returned close to the baseline, isocitrate is injected for another ICDH reaction.

tion. This enables easy cycling between the ICDH reaction and the regeneration reaction in a closed system.

ICDH and thionine were co-encapsulated in a silica gel, which was aged and then incubated with $NADP^+$. The thionine concentration was increased from previous experiments to reduce the time required to oxidize the NADPH. Isocitrate was injected into the sample at four different times. As seen in Figure 7, at each injection time the ICDH reaction is observed by the production of NADPH fluorescence. The NADPH fluorescence increases with time and levels off, at which point the ICDH reaction is assumed to be at equilibrium. These curves are consistent with those observed for gels doped only with ICDH. Between each enzymatic reaction, the encapsulated thionine was excited until the NADPH fluorescence levels returned to close to baseline. This regeneration required about 200 s of excitation each time.

The raw data shown in Figure 7 were used to estimate the NADPH produced after each isocitrate injection. The fluorescence measurements were converted to NADPH concentration by using a linear calibration curve and the background was subtracted from each enzyme reaction. Figure 8 shows the minimum and maximum adjusted NADPH concentrations for each enzyme reaction over the four cycles. Figures 7 and 8 demonstrate the ability to cycle between the enzymatic reduction of $NADP^+$ to NADPH by ICDH and the photochemical oxidation of NADPH to $NADP^+$ by thionine.

The four isocitrate injections were of decreasing isocitrate concentration. Figure 9 shows the relationship between the maximum NADPH produced as a function of the isocitrate concentration. A linear relationship between NADPH production and isocitrate concentration was observed for the investigated range. This experimental relationship is useful for sensor calibration. The physical meaning of this relationship is more difficult to understand, however, because it is not clear how well separated the two coupled reactions are in time. Overlap of the reactions and therefore simultaneous reduction of $NADP^+$ by ICDH and oxidation of NADPH by thionine are likely to complicate the net NADPH profile. Further exploration of the overlap will be required for the design of optimized continuous sensors.

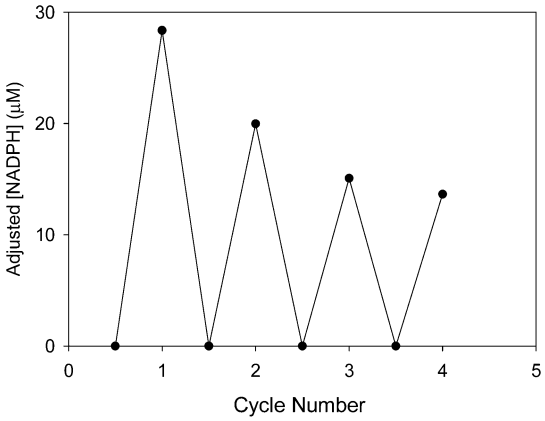

Figure 8. Adjusted NADPH concentration as a function of cycle number. The NADPH concentration was estimated based on the NADPH fluorescence measurements. The concentration was adjusted by background subtraction for each cycle. The injected isocitrate concentration decreased with cycle number resulting in a smaller NADPH production.

The data presented in Figures 7, 8, and 9 support the potential use of this coupled photochemical and enzymatic system for repeated measurements with an enzyme-doped gel without any additional washing steps or added reagents. The coupling of the two reactions was not explored beyond four cycles. Optimized sensor design may require further work to understand any potential effects of the presence of the excited thionine on the enzyme and the enzyme kinetics.

4. Conclusions

We have demonstrated that excited thionine reacts with NADPH resulting in thionine quenching and oxidation of the NADPH to $NADP^+$. In addition we have demonstrated that the reactions can be conducted in the sol−gel environment allowing for photochemical coenzyme regeneration in the sol−gel matrix. The reaction rates have been characterized both in solution and in the sol−gel monoliths. The rates are 1 to 2 orders of magnitude slower in the bulk gel. The reasons for this reduction are unknown, but it is possible that a transition to thin films may improve the reaction velocities.

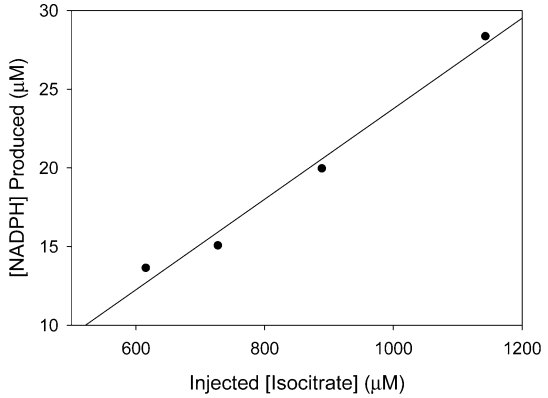

Figure 9. Calibration curve generated from repeated measurements, using the same ICDH-doped gel. The maximum NADPH concentration produced during each cycle is plotted as a function of isocitrate concentration. The line is the linear regression of the data points.

The extension of the thionine NADH reaction to NADPH opens the possibility of using thionine as a general coenzyme regeneration strategy for dehydrogenases that use either or both forms of the enzyme cofactor. The level of excited thionine can control the reaction rate. Therefore, the pattern and intensity of thionine excitation provides a design parameter that can be controlled externally in a functioning sensor.

Acknowledgment. The authors greatly appreciate the support of their research through the following: the NIH Morris K. Udall Center of Excellence for Parkinson's Disease Research (P50NS38369) and the NSF (DMR 0103952). The authors thank Dr. Esther Lan for her help in preparing the manuscript.

References and Notes

(1) Arnold, M. *Anal. Chem.* **1985**, *57*, 565.
(2) Sharma, A. *Spectrochim. Acta* **1992**, *48*, 647.
(3) Sharma, A. *Spectrochim. Acta* **1992**, *48A*, 893.
(4) Archer, M. D.; Ferreira, M. I. C.; Porter, G.; Tredwell, C. J. *Nouv. J. Chim.* **1977**, *1*, 9.
(5) Lehninger, A. L.; Nelson, D. L.; Cox, M. M. *Principles of Biochemistry*, 2nd ed.; Worth Publishers: New York, 1993.
(6) Dave, B. C.; Dunn, B.; Valentine, J. S.; Zink, J. I. *Anal. Chem.* **1994**, *66*, 1120A.
(7) Dunn, B.; Zink, J. I. *Chem. Mater.* **1997**, *9*, 2280.
(8) Rickus, J. L.; Dunn, B.; Zink, J. I. Optically Based Sol−Gel Biosensor Materials. In *Optical Biosensors*: *Present and Future*; Ligler, F. S., Rowe-Taitt, C. A., Eds.; Elsevier: Amsterdam, The Netherlands, 2002; p 427.
(9) Avnir, D.; Braun, S.; Lev, O.; Ottolenghi, M. *Chem. Mater*. **1994**, *6*, 1605.
(10) Gill, A.; Ballesteros, A. *J. Am. Chem. Soc.* **1998**, *120*, 8587.
(11) O'Neill, H.; Angley, C. V.; Hemery, I.; Evans, B. R.; Dai, S.; Woodward, J. *Biotechnol. Lett.* **2002**, *24*, 783.
(12) Yamanaka, S. A.; Dunn, B.; Valentine, J. S.; Zink, J. I. *J. Am. Chem. Soc* **1995**, *117*, 9095.
(13) Ramanathan, K.; Kamalasanan, M. N.; Malhotra, B. D.; Pradhan, D. R.; Chandra, S. *J. Sol-Gel Sci. Technol.* **1997**, *10*, 309.
(14) Chaubey, A.; Singh, G. M.; Malhotra, V. S. *Appl. Biochem. Biotechnol.* **2001**, *96*, 293.
(15) Li, C.-I.; Lin, Y.-H.; C.-L.; S.; Tsaur, J.-P.; Chau, L.-K. *Biosens. Bioelectron.* **2002**, *17*, 323.
(16) Williams, A. K.; Hupp, J. T. *J. Am. Chem. Soc.* **1998**, *20*, 4366.
(17) Ramesh, P.; Sivakumar, P.; Sampath, S. *J. Electroanal. Chem.* **2002**, *528*, 82.
(18) Ellerby, L. M.; Nishida, C. R.; Nishida, F.; Yamanaka, S. A.; Dunn, B.; Valentine, J. S.; Zink, J. I. *Science* **1992**, *255*, 1113.
(19) Miller, J. M.; Dunn, B.; Valentine, J. S.; Zink, J. I. *J. Non-Cryst. Solids* **1996**, *202*, 279.
(20) Lee, J. Immobilized Enzyme. In *Biochemical Engineering*; Prentice Hall: Upper Saddle River, NJ, 1992; p 54.
(21) Shuler, M. L.; Kargi, F. *Bioprocess Engineering*; PTR Prentice Hall: Englewood Cliffs, NJ, 1992.
(22) Braun, S.; Shtelzer, S.; Rappoport, S.; Avnir, D.; Ottolenghi, M. *J. Non-Cryst. Solids* **1992**, *147&148*, 739.
(23) Rickus, J. L.; Lan, E.; Tobin, A. J.; Zink, J. I.; Dunn, B. *Sol−gel Optical Sensors for Glutamate*; Materials Research Society Fall Meeting, 2000, Boston, MA.
(24) Husing, N.; Reisler, E.; Zink, J. I. *J. Sol−Gel Sci. Technol.* **1999**, *15*, 57.
(25) Wang, R.; Narang, U.; Prasad, P. N.; Bright, F. V. *Anal. Chem.* **1993**, *65*, 2671.
(26) Krihak, M.; Shahriari, M. R. *Opt. Mater*. **1996**, *5*, 301.
(27) Lai, W. C.; Dixit, N. S.; Mackay, R. A. *J. Phys. Chem.* **1984**, *88*, 5364.
(28) Tuite, E.; Kelly, J. M.; Beddard, G. S.; Reid, G. S. *Chem. Phys Lett.* **1994**, *226*, 517.
(29) Tuite, E.; Kelly, J. M. *Biopolymers* **1995**, *35*, 419.
(30) Carraway, E. R.; Demas, J. N.; DeGraff, B. A.; Bacon, J. R. *Anal. Chem.* **1991**, *63*, 337.
(31) Draxler, S.; Lippitsch, M. E.; Klimant, I.; Kraus, H.; Wolfbeis, O. S. *J. Phys. Chem* **1995**, *99*, 3162.
(32) Demas, J. N.; DeGraff, B. A.; Xu, W. *Anal. Chem* **1995**, *67*, 1377.
(33) Shen, C.; Kostic, N. M. *J. Am. Chem. Soc.* **1997**, *119*, 1304.
(34) Castellano, F. N.; Meyer, G. J. *J. Phys. Chem* **1995**, *99*, 14742.
(35) Sharma, A.; Quantrill, N. S. M. *Spectrochim. Acta* **1994**, *50A*, 1179.
(36) Sharma, A.; Quantrill, N. S. M. *Spectrochim. Acta* **1994**, *50A*, 1161.
(37) Sharma, A.; Quantrill, N. S. M. *Biotechnol. Prog.* **1996**, *12*, 413.
(38) Stryer, L. *Biochemistry*, 3rd ed.; W. H. Freeman and Company: New York, 1988.